

SANDIA REPORT

SAND2006-7709

Unlimited Release

Printed December 2006

LDRD Final Report on "Controlled Synthesis of Nanocrystalline Catalysts - from Solutions to Supports" (LDRD 104111)

Richard A. Kemp, Michael Lattman, Shawn P. Resler, Vernal Richards,
and William E. Buhro

Prepared by
Sandia National Laboratories
Albuquerque, New Mexico 87185 and Livermore, California 94550

Sandia is a multiprogram laboratory operated by Sandia Corporation,
a Lockheed Martin Company, for the United States Department of Energy's
National Nuclear Security Administration under Contract DE-AC04-94AL85000.

Approved for public release; further dissemination unlimited.



Issued by Sandia National Laboratories, operated for the United States Department of Energy by Sandia Corporation.

NOTICE: This report was prepared as an account of work sponsored by an agency of the United States Government. Neither the United States Government, nor any agency thereof, nor any of their employees, nor any of their contractors, subcontractors, or their employees, make any warranty, express or implied, or assume any legal liability or responsibility for the accuracy, completeness, or usefulness of any information, apparatus, product, or process disclosed, or represent that its use would not infringe privately owned rights. Reference herein to any specific commercial product, process, or service by trade name, trademark, manufacturer, or otherwise, does not necessarily constitute or imply its endorsement, recommendation, or favoring by the United States Government, any agency thereof, or any of their contractors or subcontractors. The views and opinions expressed herein do not necessarily state or reflect those of the United States Government, any agency thereof, or any of their contractors.

Printed in the United States of America. This report has been reproduced directly from the best available copy.

Available to DOE and DOE contractors from
U.S. Department of Energy
Office of Scientific and Technical Information
P.O. Box 62
Oak Ridge, TN 37831

Telephone: (865) 576-8401
Facsimile: (865) 576-5728
E-Mail: reports@adonis.osti.gov
Online ordering: <http://www.osti.gov/bridge>

Available to the public from
U.S. Department of Commerce
National Technical Information Service
5285 Port Royal Rd.
Springfield, VA 22161

Telephone: (800) 553-6847
Facsimile: (703) 605-6900
E-Mail: orders@ntis.fedworld.gov
Online order: <http://www.ntis.gov/help/ordermethods.asp?loc=7-4-0#online>



SAND2006-7709
Unlimited Release
Printed December 2006

**“Controlled Synthesis of Nanocrystalline Catalysts –
from Solutions to Supports”
(LDRD 104111)**

Richard A. Kemp and Michael Lattman
Ceramic Processing and Inorganic Materials (01815)
Sandia National Laboratories
P.O. Box 5800
Albuquerque, NM 87185-1349

Shawn P. Resler, Vernal Richards, and William E. Buhro
Department of Chemistry
Washington University in St. Louis
St. Louis, MO 63130-4899

Abstract

Control of nanoparticle size is crucial to the development of nanotechnology. At this point in time, no general, rational synthetic strategy for controlling nanocrystal diameters and producing narrow diameter distributions has emerged. This is a reflection of a poor understanding of the mechanisms for nanocrystal growth. Based on previous studies of bismuth and gold nanoparticle growth, this work clearly establishes two new synthetic approaches to controlled growth of colloidal Pt nanocrystals, both based on aggregative-growth mechanisms, which afford narrow size distributions and size control over a wide and relevant size regime. The first new method is a phase transfer process, where growth is controlled by varying ligand stabilizer concentrations. The second method involves rapid reduction of a molecular platinum precursor in the presence of a polymer stabilizer.

At present the size control is empirical, and incompletely understood and incompletely developed. However, the new synthetic pathways are amenable to kinetic study and analysis, establishing that a quantitative, rational control of sizes and size distributions can be achieved.

Contents

	<u>Page</u>
Listing of Figures	6
I. Introduction	
A. <i>Overview</i>	7
B. <i>Background</i>	7
II. Preliminary Studies	8
III. Results and Discussion.....	11
IV. Conclusions.....	16
V. References.....	17
Distribution	19

Listing of Figures

	Page
Figure 1. TEM images (scale bars = 50 nm). (a) bimodal distribution of Bi nanocrystals; (b) post-growth Bi nanocrystals; (c) Au nanocrystals; (d) post-growth Au nanocrystals.	9
Figure 2. Kinetic data (points) for the aggregative growth of nanocrystals. The curves are calculated fits using eq 1. (a) Bi nanocrystals. (b) Au nanocrystals; data were collected at the salt concentrations (molarity) given in the inset.	10
Figure 3. Pt nanocrystals grown by the polyol method; $D_{ave} = 2.43 \pm 0.55$ nm.	12
Figure 4. (a) pre-synthesized primary Pt nanocrystallites, $d = 2.0 \pm 0.8$ nm; (b) Pt nanocrystals formed by controlled coarsening, $d = 6.1 \pm 1.2$ nm.	13
Figure 5. Evolution of experimental nanocrystal-size distributions in time under controlled coarsening.	13
Figure 6. TEM images from rapid primary Pt particle generation obtained: (a) at 20 min; (b) 240 min. Final $d = 9.1 \pm 1.2$ nm.	14
Figure 7. Nanocrystal-size distributions during aggregative growth after rapid primary Pt-nanocrystal generation.	15
Figure 8. Kinetic profile for the growth of Pt nanocrystals from $\text{Pt}(\text{acac})_2$. (■) average diameter measured from the nanocrystal-size distributions; (—) sigmoidal fit as a guide for the eye.	16

Introduction

A. Overview

Control of nanoparticle size is crucial to the development of nanotechnology. At this point in time, no general, rational synthetic strategy for controlling nanocrystal diameters and producing narrow diameter distributions has emerged. This is a reflection of a poor understanding of the mechanisms for nanocrystal growth. The long-term goal of this project is to develop a detailed understanding of the growth process of nanocrystals and to apply this knowledge to produce, predictably and in a reproducible manner, nanoparticles of a specific size and size distribution of a wide variety of materials.

Due to the short duration of this project, efforts were concentrated on the synthesis and growth of platinum nanocrystals. Our initial studies began with the preparation of colloidal Pt nanocrystals and succeeded in reaching several goals:

- Survey and develop Pt-nanocrystal syntheses for systematic variation of nanocrystal size while maintaining narrow size distributions over a range of catalytically relevant diameters (ca. 2-10 nm)
- Identify preparative pathways and **controlled** aevastation strategies to allow quantitative kinetic analysis of nanocrystal growth
- Look for and promote aggregative-growth mechanism.

B. Background

Nanocrystalline materials exhibit a range of unusual optical, electrical, and chemical properties that are of great interest for applications in sensing, labeling, catalysis, electronics, optics, multifunctional composites, etc.¹ Nanocrystal properties are generally size dependent, requiring narrowly dispersed specimens over a range of mean diameters for systematic

experimental studies and certainly for optimum application. Thus, the production of near-monodisperse nanocrystal materials has long been a key synthetic criterion.² Unfortunately, a general, rational strategy for controlling nanocrystal diameters and producing narrow size distributions has not emerged. This is a reflection of a poor understanding of the mechanisms for nanocrystal growth. Particle aggregation has long been recognized as a contributing mechanism to the growth of micrometer-sized colloidal materials; however, the possible role of aggregation processes in nanocrystal growth has been *largely ignored*. **We argue that aggregative nanocrystal growth is more common than has been appreciated, and that aggregative growth has intrinsic advantages that can be exploited for achieving diameter and dispersity control in nanocrystal synthesis.**

II. Preliminary Studies

We have separately established aggregative-growth mechanisms for near-monodisperse Au and Bi nanocrystals.³ Solution-phase decomposition of $\text{Bi}[\text{N}(\text{SiMe}_3)_2]_3$ produces narrowly dispersed Bi nanocrystals with mean diameters in the range of 5 – 25 nm, depending on reaction conditions. TEM images obtained very early in the process reveal bimodal size distributions comprising primarily very small ($d < 2$ nm) Bi nanocrystals, with a few larger nanocrystals (Fig. 1a). Over time the larger particles grow at the expense of the smaller particles, until the latter are consumed (Fig. 1b). These results are consistent with aggregative growth. As a second example, the solution-based thermal ripening of small, polydisperse Au nanocrystals ($d \leq 2$ nm; Fig. 1c) affords larger, near-monodisperse Au nanocrystals having mean diameters in the range of 5 – 10 nm (Fig. 1d).

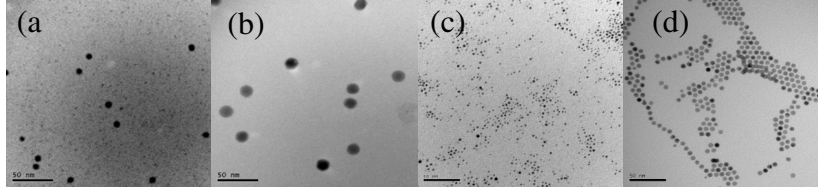


Figure 1. TEM images (scale bars = 50 nm). (a) bimodal distribution of Bi nanocrystals; (b) post-growth Bi nanocrystals; (c) Au nanocrystals; (d) post-growth Au nanocrystals.

In addition to the evidence in Figure 1, studies of growth kinetics by us and by others have generally found sigmoidal growth curves consistent with aggregative-growth mechanisms.⁴ As such, in Equation 1, we have adapted the well-known KJMA model⁵ to the kinetic analysis of aggregative growth by redefining nucleation to be the formation (and coalescence) of a critical aggregate.

$$\frac{M(t)}{M_{lim}} = \frac{1}{1 + \exp\left(-\frac{t - k_n^{-1}}{\Delta t_n}\right)} \left(1 - \exp\left(-\left(k_g t\right)^d\right)\right) + k_{OR} t \quad (1)$$

In this expression, $M(t)$ and M_{lim} are the average nanocrystal mass at time t and the limiting (final) average mass at the end of growth, respectively. These quantities are experimentally determined by analysis of TEM images. The quantity k_n is the maximum nucleation rate, and Δt_n is the width of the time window for nucleation. These are extracted from nanocrystal size distributions measured from TEM images. The exponent d is the growth dimension, which is conventionally assigned the value 3 for 3D nucleation-limited growth, and 1.33 for diffusion-limited growth, applicable when k_n becomes very fast.⁶ The quantities k_g and k_{OR} are the growth rate and equilibrium Ostwald-ripening rate, respectively. They are obtained by fitting eq 1 to the experimental kinetic data ($M(t)/M_{lim}$) vs. t) using the well-known Origin graphing and function-fitting software package, which is widely accessible and widely used. In

modifying Equation 1 and the mechanistic model it represents, we have redefined nucleation and growth to apply to aggregative processes (see above), developed a method for directly evaluating k_n and Δt_n from experimental data (not detailed here), and added an Ostwald-ripening term.

Kinetic data for the aggregative growth of Bi and Au nanocrystals are shown in Figure 2. The fits to eq. 1 are good, affording experimental determination of the nucleation time window Δt_n and the rate constants k_n , k_g , and k_{OR} . For the Au nanocrystals (Fig. 2b), the maximum nucleation rate for critical-aggregate formation (k_n) was found to be highly sensitive to the concentration of an added salt, $[(n\text{-octyl})_4\text{N}]\text{Br}$. The results indicate that alkanethiol-capped Au nanocrystals, which are generally presumed to be sterically stabilized, are in fact partially electrostatically stabilized. Addition of salt collapses the electrical double layer surrounding the nanocrystals, decreasing the barrier for their aggregation and coalescence. We found that the magnitude of k_n varied with salt concentration over ca. two orders of magnitude (Fig. 2b).

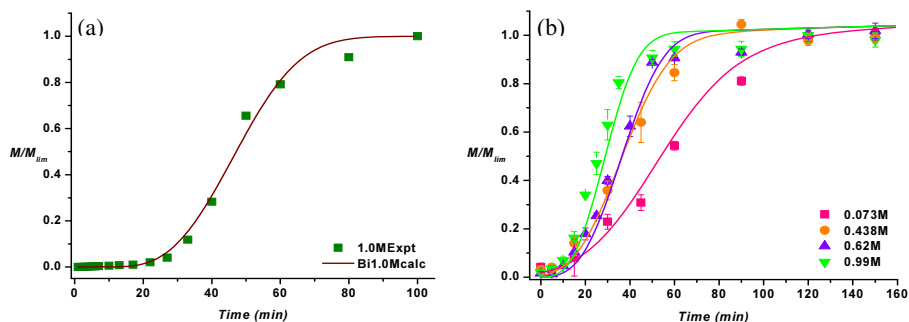


Figure 2. Kinetic data (points) for the aggregative growth of nanocrystals. The curves are calculated fits using eq 1. (a) Bi nanocrystals. (b) Au nanocrystals; data were collected at the salt concentrations (molarity) given in the inset.

The ability to systematically vary the aggregative nucleation rate k_n provides *the* important control element for nanocrystal synthesis. As k_n increases relative to k_g , the induction period shrinks and essentially disappears, and a crossover from nucleation-limited to diffusion-limited growth is realized. At this crossover point ($k_n \approx 20k_g$), theory indicates that the final size distribution will be the narrowest achievable (standard deviation $\approx 5\text{-}7\%$ of the mean diameter), and the final mean nanocrystal size will be the largest achievable, for a given temperature and precursor concentration. Our results with Au nanocrystals bear out these predictions; the largest diameters and narrowest diameter distributions are achieved at the salt concentration (0.99 M) that produces crossover-point kinetics. We obtain smaller nanocrystals, without a large increase in the size distribution, by systematically decreasing k_n .

III. Results and Discussion

We began by evaluating existing methods for colloidal-Pt-nanocrystal synthesis. Only two reliable methods have been reported. The first is the reduction of a Pt salt by a borohydride or organoaluminum reagent.⁷ The second is referred to as the “polyol” method, where $\text{Pt}(\text{acac})_2$ is reduced by an alkanediol with heating.⁸ Both methods reliably yield 2-3 nm particles with modestly narrowed dispersities ($\pm 40\%$ and 25% , respectively). A third method, in which Pt salts are reduced by H_2 , was not pursued by us due to its tendency to yield significant amounts of agglomerated metal in addition to colloidal nanocrystals.⁹

In our hands the polyol method yielded results generally consistent with literature reports. The nanocrystals showed *no tendency towards aggregation*, as shown in Figure 3. These nanocrystals were also resistant to thermal-ripening procedures intended to produce larger, controlled nanocrystal sizes. The maximum size available by this method was limited to diameters of ~ 3 nm, without the use of multiple precursor additions,¹⁰ which were impractical.

Our experimental work established that the polyol-derived Pt nanocrystals exhibited unusual stability toward aggregative growth and Ostwald ripening, so this synthetic method was abandoned.

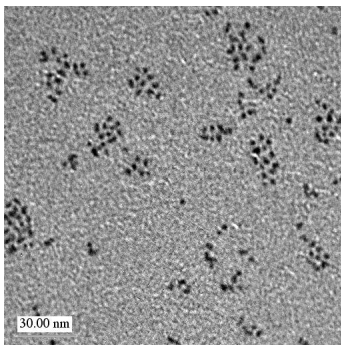


Figure 3. Pt nanocrystals grown by the polyol method; $D_{ave} = 2.43 \pm 0.55$ nm.

We subsequently developed two syntheses that allowed controlled growth of Pt nanocrystals within the desired size range (diameters = 2-10 nm). The first new synthesis was a controlled-coarsening procedure using small, primary, Pt nanocrystallites (ca. 2 nm) prepared by a phase-transfer procedure. This method is analogous to that for Au-nanocrystal synthesis mentioned in the previous section. The primary nanocrystallites were stabilized by tetraoctylammonium bromide (TOABr) and dodecylamine (DDA), and were easily stored and manipulated. Controlled coarsening through aggregative growth of these nanocrystals was induced thermally in appropriate solvents, by adding various concentrations of additional TOABr.

We have identified boundary TOABr concentrations that distinguish three different growth regimes. At low TOABr concentration only Ostwald ripening occurs, and the 2-nm primary particles can be grown to about 3.5 nm with a significant broadening of the size distribution. At intermediate TOABr concentrations, controlled aggregative growth with nanocrystal coalescence occurs, which is a desirable growth mechanism. At high TOABr concentrations, aggregation occurs but *not* coalescence, producing aggregates of primary nanocrystals. The latter growth

regime is not synthetically useful, but has great mechanistic significance in that it provides direct evidence for the participation of aggregative processes during growth. Figure 4 shows Pt nanocrystals grown under the synthetically useful intermediate conditions, where the primary nanocrystals grow by aggregation to 6-nm diameters, while maintaining respectable (but unoptimized) size distributions. Figure 5 illustrates the evolution of the nanocrystal-size distributions during the reaction, demonstrating that the controlled-coarsening procedure will provide a successful preparation of narrowly dispersed Pt nanocrystals in the desired size range (2-10 nm).

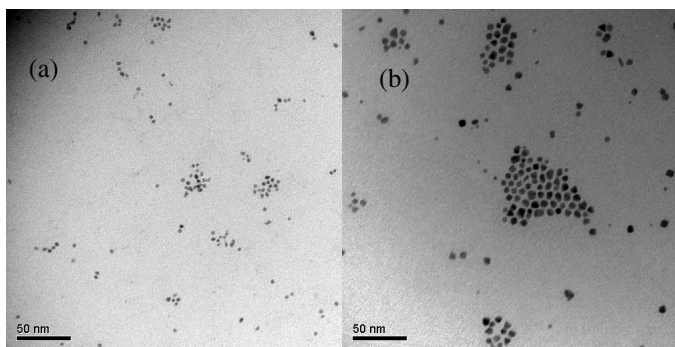


Figure 4. (a) pre-synthesized primary Pt nanocrystallites, $d = 2.0 \pm 0.8$ nm; (b) Pt nanocrystals formed by controlled coarsening, $d = 6.1 \pm 1.2$ nm.

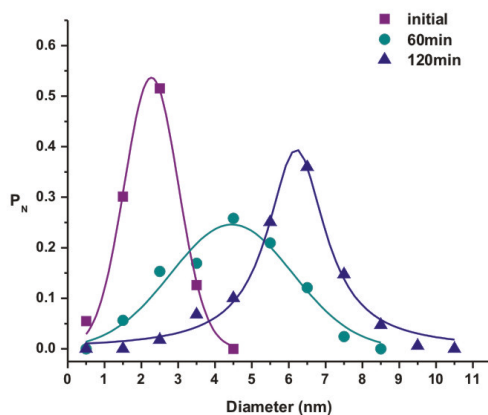


Figure 5. Evolution of experimental nanocrystal-size distributions in time under controlled coarsening.

We have also developed a second new Pt-nanocrystal synthesis by rapid primary particle generation. In this approach, small primary Pt nanocrystals are rapidly generated from a molecular precursor, which subsequently undergo aggregative growth affording larger, narrowly dispersed Pt nanocrystals. In this procedure, Pt(acac)₂ is reduced by octadecanethiol (ODT) in the presence of a polymer stabilizer, polyvinylpyrrolidene-co-hexadecene (PVP-co-PHD) in an appropriate solvent. The strategy is closely analogous to our previous synthesis of Bi nanocrystals mentioned in the previous section. Figure 6a reveals the generation of many ~1.5-nm primary Pt particles after a 20-min reaction time, along with a much smaller fraction of 5-6 nm particles, which are beginning to form and grow by an aggregative process that consumes the smaller particles. After 2 hours, nanocrystals with an average diameter of 8 nm are observed, with gradual growth up to 9 nm at 4 hours (Figure 6b). The evolution of the measured nanocrystal-size distributions is shown in Figure 7.

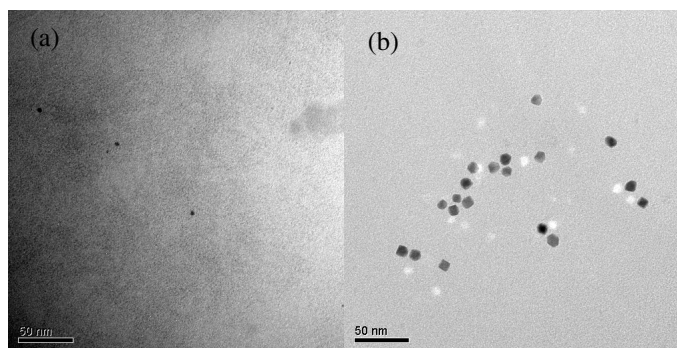


Figure 6. TEM images from rapid primary Pt particle generation obtained: (a) at 20 min; (b) 240 min. Final $d = 9.1 \pm 1.2$ nm.

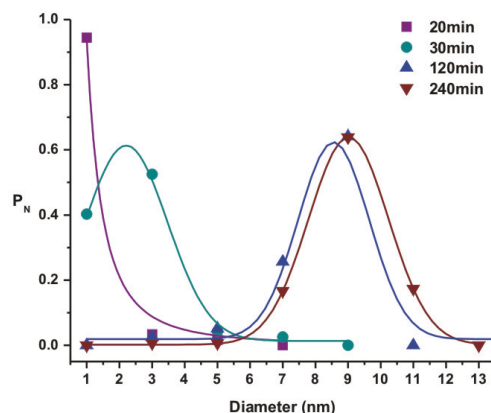


Figure 7. Nanocrystal-size distributions during aggregative growth after rapid primary Pt-nanocrystal generation.

The growth kinetics for this process, plotted in Figure 8 using the Figure 7 data, constitute an extremely positive and exciting result. Figure 8 reveals an initial induction period, followed by rapid aggregative growth, and then *very slow* Ostwald ripening. That is, the preliminary growth kinetics are very consistent with a controlled, aggregative-growth process, as we have been seeking in this proposed effort. The observation of very slow Ostwald ripening is a synthetically useful outcome because it indicates that the ultimate nanocrystal size will be determined by the aggregative-growth regime, which is amenable to chemical control. Although not yet developed and optimized, the early indications for this growth method strongly suggest it will afford narrow size distributions and controlled Pt-nanocrystal diameters in the catalytically relevant size range of 2-10 nm.

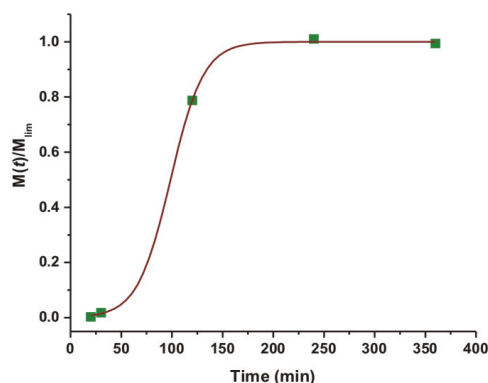


Figure 8. Kinetic profile for the growth of Pt nanocrystals from $\text{Pt}(\text{acac})_2$. (■) average diameter measured from the nanocrystal-size distributions; (—) sigmoidal fit as a guide for the eye.

IV. Conclusions

The results from our efforts clearly establish two new synthetic approaches to colloidal Pt nanocrystals, both based on aggregative-growth mechanisms, which afford narrow size distributions and size control over a wide and relevant size regime. At present the size control is empirical, and incompletely understood and incompletely developed. However, the new synthetic pathways are amenable to kinetic study and analysis, as is shown by Figure 8, establishing that a quantitative, rational control of sizes and size distributions can be achievable. These are extremely successful and promising results, because they suggest that after many years of empirical Pt-nanocrystal synthesis with only modest control over nanocrystal sizes, a rational basis for synthetic control will soon be in hand.

V. References

- ¹ (a) Luo, X.; Morrin, A.; Killard, A. J.; Smyth, M. R. *Electroanalysis* **2006**, *18*, 319; (b) Franke, M. E.; Koplín, T. J.; Simon, U. *Small*, **2006**, *2*, 36; (c) Prinz, G.A. *Science* **1998**, *282*, 1660; (d) Turner, A. P. *Science* **2000**, *290*, 1315; (e) Wolfbeis, O. S. *J. Mater. Chem.* **2005**, *15*, 2657.
- ² (a) Franke, M. E.; Koplín, T. J.; Simon, U. *Small* **2006**, *2*, 36; (b) Yin, Y.; Alivisatos, A. P. *Nature* **2005**, *437*, 664; (c) Park, J. ; An, K.; Hwang, Y.; Park, J. G.; Noh, H. J.; Kim, J. Y.; Park, J. H.; Hwang, N. M.; Hyeon, T. *Nature Mater.* **2004**, *3*, 891; (d) Burda, C.; Chen, X.; Narayanan, R.; El-Sayed, M. A. *Chem. Rev.* **2005**, *105*, 1025.
- ³ Unpublished results from the laboratories of William E. Buhro, Washington University.
- ⁴ (a) Watzky, M. A.; Finke, R. G. *J. Am. Chem. Soc.* **1997**, *119*, 10382; (b) Besson, C.; Finney, E. E.; Finke, R. G. *J. Am. Chem. Soc.* **2005**, *127*, 8179; (c) Besson, C.; Finney, E. E.; Finke, R. G. *Chem Mater.* **2005**, *17*, 4925; (d) Mantzaris, N. V. *Chem. Eng. Sci.* **2005**, *60*, 4749. (a) Schwartzer, H.-C.; Peukert., W. *Chem. Eng. Sci.* **2005**, *60*, 11; (e) Ding, A.; Houslow, M. J.; Biggs, C. A. *Chem. Eng. Sci.* **2006**, *61*, 63
- ⁵ Gualtieri, A. F. *Phys. Chem. Minerals* **2001**, *28*, 719.
- ⁶ (a) Yang, J.; McCoy, B. J. *J. Chem. Phys.* **2005**, *122*, 244905; (b) Crespo, D.; Pradell, T.; Clavaguera-Mora, M. T.; Clavaguera, N. *Phys. Rev. B*, **1997**, *55*, 3435; (c) Pradell, T.; Crespo, D.; Clavaguera, N.; Clavaguera-Mora, M. T. *J. Phys.: Condens. Matter* **1998**, *10*, 3833.
- ⁷ Angermund, K.; Buhl, M.; Dinjus, E.; Endruschat, U.; Gassner, F.; Haubold, H.-G.; Hormes, J.; Kohl, Gesa; Mauschick, F. T.; Modrow, H.; Mortel, R.; Mynott, R.; Tesche, B.; Vad, T.; Waldofner, N.; Bonnemann, H. *Angewandte Chemie, International Edition* **2002**, *41*, 4041-4044.
- ⁸ Sobal, N. S.; Ebels, U.; Moehwald, H.; Giersig, M. *Journal of Physical Chemistry B* **2003**, *107*, 7351-7354.
- ⁹ Besson, C.; Finney, E. E.; Finke, R. G. *Journal of the American Chemical Society* **2005**, *127*, 8179-8184.
- ¹⁰ Qiu, L.; Liu, F.; Zhao, L.; Yang, W.; Yao, J. *Langmuir* **2006**, *22*, 4480-4482.

INITIAL DISTRIBUTION

10	MS1349	R.A. Kemp
1	MS1349	J.E. Miller
1	MS1349	C.A. Stewart
1	MS1349	W.F. Hammetter
1	MS0887	D.B. Dimos
1	MS0323	Donna Chavez, Org. 1011 (electronic only)
1	MS0899	Technical Library, 9536 (electronic only)



Sandia National Laboratories